A curvilinear generalization of the Yamanaka-Ankersen state transition matrix

Alicia Martínez-Cacho*[1] and Claudio Bombardelli†[1]

[1]Grupo de Dinámica Espacial, Universidad Politécnica de Madrid, Spain

1 Introduction

The work of Yamanaka and Ankersen (hereafter YA) in [1] represents a breakthrough in the modelling of relative motion along close Keplerian orbits. In that paper, the authors were able to obtain a fully analytical state transition matrix (STM) starting from the linearized equations of relative motion with respect to a Keplerian elliptical orbit, also known as Tschauner-Hampel (TH) equations. Since that proposed STM works for an arbitrary value of the nominal orbit eccentricity it is considered a milestone result in astrodynamics and is widely employed in the literature. A fundamental, often overlooked, step in the derivation of the YA STM, is the use of a "pulsating" reference length unit very similar to the one employed in the Nechvile curvilinear coordinates for the study of the restricted three-body problem.

In this work, we rewrite the relative motion equations in pulsating cylindrical coordinates, then linearize them obtaining a curvilinear analogue of the TH equations, and finally obtain a curvilinear analogue of the YA STM. The advantage of working with curvilinear coordinates instead of Cartesian ones has already been analyzed, for example in [2][3] for a circular case with a cylindrical system, and in [4] for an elliptical orbit with a spherical one. Here, we apply the cylindrical coordinates STM to the propagation of orbit uncertainties showing an improvement in uncertainty realism compared to the Cartesian case in the great majority of relevant space situational awareness applications.

2 Curvilinear system definition

Let us use the distance from the target to the central body in each instant of time, $R = p/\gamma(\nu)$, as a pulsating unit of distance, where $\gamma(\nu) = 1 + e\cos\nu$ and $p = a(1-e^2)$, being a, e and ν the semi-major axis, eccentricity and true anomaly of the target's orbit, respectively. Using this, we define the in-plane curvilinear coordinates, that appear on Figure 1, as:[1]

$$\rho = \sqrt{(1+x)^2 + (y)^2} - 1, \tag{1}$$

$$\theta = atan2^*(y, 1+x), \tag{2}$$

where the position of the chaser relative to the target in the local-horizontal (LVLH) frame, with the orthonormal basis $\{\mathbf{i}, \mathbf{j}, \mathbf{k}\}$ (Figure 1)[2], is:

$$\mathbf{d} = x\mathbf{i} + y\mathbf{j} + z\mathbf{k}. \tag{3}$$

The out-of-plane curvilinear coordinate coincides with the Cartesian one, that is, the mentioned z.

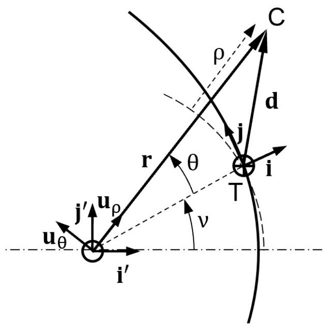

Figure 1: Relative motion geometry using the instant radious of the target as the unit of distance.

3 State transition matrix in curvilinear coordinates

First of all, we need the equations of motion in the curvilinear coordinates. These are:

$$\begin{cases} \rho'' - 2\theta' - \dfrac{3}{\gamma}\rho = a_{i\rho} + \dfrac{1}{\gamma}a_{g\rho} \\ \theta'' + 2\rho' = a_{i\theta} \\ z'' + z = \dfrac{1}{\gamma}a_{gz}, \end{cases} \tag{4}$$

*Email: alicia.martinez.cacho@upm.es. Research supported by a PhD grant under UPM "Programa Propio".

†Email: claudio.bombardelli@upm.es. Research supported by MINECO/AEI and FEDER/EU under Project PID2020-112576GB-C21. The authors thank the MINECO/AEI of Spain for their financial support.

[1]The function $atan2^*$ is $\mod(atan2(x,y) + 2\pi, 2\pi)$.

[2]Notice that the basis $\{\mathbf{i}', \mathbf{j}', \mathbf{k}'\}$ corresponds to the perifocal coordinate system.

where the right side contains the non-linear terms:

$$
\begin{aligned}
a_{i\rho} &= {\theta'}^2(1+\rho) + 2\theta'\rho, \\
a_{g\rho} &= -2\rho + 1 - \frac{(1+\rho)}{\left[(1+\rho)^2 + z^2\right]^{3/2}}, \\
a_{i\theta} &= \frac{2\rho'(\rho - \theta')}{1+\rho}, \\
a_{gz} &= z - \frac{z}{\left[(1+\rho)^2 + z^2\right]^{3/2}}.
\end{aligned} \tag{5}
$$

These equations are obtained following a procedure similar to the one used in [2], but with an elliptical orbit for the target instead of a circular one. The true anomaly of the target is used as the independent variable (whose derivatives are indicated with primes).

The linearized version of these equations has the same structure as the TH equations:

$$
\begin{cases}
\rho'' - 2\theta' - \dfrac{3}{\gamma}\rho = 0 \\
\theta'' + 2\rho' = 0 \\
z'' + z = 0.
\end{cases} \tag{6}
$$

This similarity allows us to obtain a STM similar to the YA one by following the same mathematical development followed in [1]. Hence, the problem has to be subdivided in the out-of-plane and in-plane motions.

3.1 Out-of-plane

In the out-of-plane motion, curvilinear and Cartesian coordinates coincide. [3] Therefore, the STM coincides too, being:

$$
\begin{bmatrix} z \\ z' \end{bmatrix} = \frac{1}{\gamma_{\nu-\nu_0}} \begin{bmatrix} c & s \\ -s & c \end{bmatrix}_{\nu-\nu_0} \begin{bmatrix} z_0 \\ z'_0 \end{bmatrix}, \tag{7}
$$

where $c = \gamma \cos\nu$ and $s = \gamma \sin\nu$.

3.2 In-plane

In this motion, cylindrical and Cartesian coordinates differ. However, as the equations have a similar structure, the curvilinear STM can be obtained following the same procedure depicted in [1]. The result is:

$$
\begin{bmatrix} \rho \\ \theta \\ \rho' \\ \theta' \end{bmatrix} = \begin{bmatrix} 0 & s & c & (2 - 3esJ) \\ -1 & c\,(1+1/\gamma) & -s\,(1+1/\gamma) & -3\gamma^2 J \\ 0 & s' & c' & -3e\left(s'J + s/\gamma^2\right) \\ 0 & -2s & -2c+e & -3\,(1-2esJ) \end{bmatrix}_{\nu} \begin{bmatrix} K_1 \\ K_2 \\ K_3 \\ K_4 \end{bmatrix} \tag{8}
$$

$$
\begin{bmatrix} K_1 \\ K_2 \\ K_3 \\ K_4 \end{bmatrix} = \frac{1}{e^2-1} \begin{bmatrix} 3e(s/\gamma)(1+1/\gamma) & e^2-1 & 2-ec & es(1+1/\gamma) \\ -3(s/\gamma)(1+e^2/\gamma) & 0 & c-2e & -s(1+1/\gamma) \\ -3(c/\gamma+e) & 0 & -s & -c(1+1/\gamma)-e \\ 3\gamma+e^2-1 & 0 & es & \gamma^2 \end{bmatrix}_{\nu_0} \begin{bmatrix} \rho_0 \\ \theta_0 \\ \rho'_0 \\ \theta'_0 \end{bmatrix}, \tag{9}
$$

[3]Notice that in [1] the coordinate y is oriented following the direction of $-\mathbf{h}$ (being $\mathbf{h}$ the angular momentum vector of the target) while in our system z is oriented towards $\mathbf{h}$.

where $J(\nu) = \int_{\nu_0}^{\nu} \frac{d\nu}{\gamma^2(\nu)} = \frac{\mu^2}{h^3}(t - t_0)$, being μ the gravitational parameter of the central body and h the angular momentum of the target.

4 Uncertainty Realism

One important application of the STM is the uncertainty propagation. Hence, it is of high interest the evaluation of the performance in uncertainty propagation of the new curvilinear STM by comparing it with the YA STM performance. This is carried out by means of the Uncertainty Realism which is evaluated using the Cramer-von Mises (CvM) test of the Mahalanobis distance distribution. The details of this test can be found in [5].

Considering an initial Gaussian Probability Density Function (PDF) and its corresponding set of orbital states sampled, the CvM test evaluates if the Mahalanobis distance of the samples follows a chi-squared distribution for each epoch. When this is achieved the PDF remains Gaussian, thus the uncertainty is realistic. The Mahalanobis distance is defined as:

$$
\mathcal{M}_i(\mathbf{x}_i; \boldsymbol{\mu}, \mathbf{P}) = (\mathbf{x}_i - \boldsymbol{\mu})^T \mathbf{P}^{-1} (\mathbf{x}_i - \boldsymbol{\mu}), \tag{10}
$$

where, at each time instance, $\mathbf{x}_i$ is the ith sample state propagated with a full nonlinear orbital dynamics model, $\boldsymbol{\mu}$ is the mean of the set of samples and $\mathbf{P}$ is the linearly[4] propagated covariance matrix. The covariance matrix propagation is done by:

$$
\mathbf{P}(t) = \mathbf{\Phi}(t, t_0)\mathbf{P}(t_0)\mathbf{\Phi}^T(t, t_0), \tag{11}
$$

where $\mathbf{\Phi}(t, t_0)$ is the STM in the corresponding space.

4.1 Test conditions

In this work, the CvM test is performed in Cartesian coordinates using YA STM and in curvilinear coordinates with the STM obtained in section 3. In both cases the set of samples has a size of $N = 10000$ and the test is performed with a 99.9% confidence level. This pair of confidence level and N implies that the covariance is realistic while the value of the CvM test statistics remains lower than 1.16204 [6]. The set of samples is propagated using Matlab's ode45 and a Keplerian dynamic model.

5 Results

There are two different orbits to be studied whose initial orbital elements are shown in Table 1 and whose initial covariance matrices written in the LVLH frame

[4]Notice that the CvM test can be used with nonlinear covariance propagation methods. However, as our interest lies on the study of a STM, only the linear propagation has been considered

are shown in Table 2. When performing the test for the curvilinear STM, the covariance matrix is transformed by the full nonlinear elements conversion.

Type	r_p (km)	e	i (°)	Ω (°)	ω (°)	M (°)
GEO	42164.1	0	0	0	0	0
LEO	7000	Variable	25	120	0	180

Table 1: Initial orbital elements

Case	σ_x (m)	σ_y (m)	σ_z (m)	$\sigma_{\dot{x}}$ (m/s)	$\sigma_{\dot{y}}$ (m/s)	$\sigma_{\dot{z}}$ (m/s)
GEO	1000	3000	5000	0.3	0.1	0.4
LEO	100	300	500	0.03	0.01	0.04

Table 2: Initial Covariance in LVLH frame

The first case of study is a GEO with a TLE-like covariance matrix. The values of the covariance matrix have been obtained after analyzing the position and velocity uncertainty for different satellites in GEO, whose data were obtained as two-line elements (TLEs) from the webpage `https://www.space-track.org/`. As for the second case, it corresponds to a LEO that is studied for different eccentricities: from the circular case to $e = 0.8$ in intervals of 0.1. For this case, the covariance matrix selected is the the GEO TLE-like covariance reduced by a factor of 10.

The Cramer-von Mises (CvM) test statistics for the circular cases, that is, the GEO and the circular LEO is shown in Figure 2. In both cases, the CvM test fails before 1 orbital period with the Cartesian YA STM whereas with the curvilinear STM the realism is maintained for more than 10 orbits for GEO and more than 16 orbits for the circular LEO. Therefore, in these cases curvilinear coordinates provides a huge improvement in realism with respect to Cartesian ones.

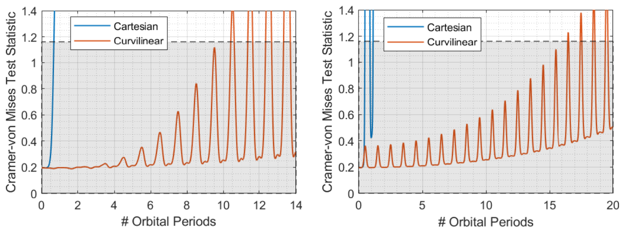

Figure 2: CvM test statistics for: left, GEO; right, circular LEO

Figure 3 shows the results for two of the eccentricities studied for the eccentric LEO: the smallest, $e = 0.1$, and the highest, $e = 0.8$. For $e = 0.1$, the realism is maintained for half an orbit for YA STM and around 4 orbits for curvilinear STM. This result entails a better performance with the curvilinear STM again. Regarding the case of $e = 0.8$, both YA and the curvilinear STM provide the same results. As we can see in the right graphics of figure 3, the test fails before 1 orbital period, which is a poor result.

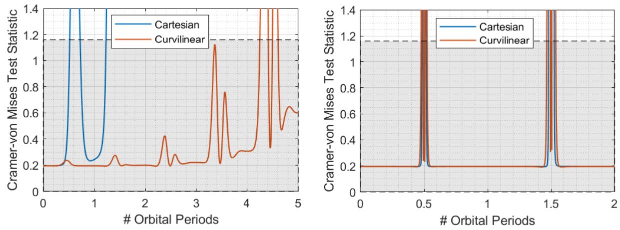

Figure 3: CvM test statistics for the LEO case with: left, $e = 0.1$; right, $e = 0.8$

	Eccentricity								
STM	0	0.1	0.2	0.3	0.4	0.5	0.6	0.7	0.8
Cart	0.47	0.52	1.32	1.38	1.42	1.45	1.46	0.49	0.48
Curv	16.48	4.25	2.37	2.35	2.37	2.4	2.42	1.47	0.48

Table 3: Number of orbital periods for the CvM test before failure for LEO

The results obtained for the rest of the eccentricities are summarized in table 3. As for the Cartesian YA STM, the realism breaks down after only half an orbit or one orbit and a half for all the cases considered. On the other hand, the curvilinear STM maintains covariance realism for a considerably higher number of orbits as long as the eccentricity is not too high. This advantage decreases as the eccentricity grows, disappearing for eccentricities higher than 0.7 where both Cartesian and curvilinear coordinates perform poorly.

References

[1] K. Yamanaka, F. Ankersen, New state transition matrix for relative motion on an arbitrary elliptical orbit, *Journal of Guidance, Control and Dynamics* **25** (2002), 60-66.

[2] C. Bombardelli, J. L. Gonzalo, J. Roa, Approximate solutions of non-linear circular orbit relative motion in curvilinear coordinates, *Celestial Mechanics and Dynamical Astronomy* **127** (2017), 49-66.

[3] D.K: Geller, T.A. Lovell, Angles-Only Initial Relative Orbit Determination Performance Analysis using Cylindrical Coordinates, *J of Astronaut Sci* **64** (2017), 72–96.

[4] C. Han et. al., A linear model for relative motion in an elliptical orbit based on a spherical coordinate system, *Acta Astronautica* **157** (2019), 465-476

[5] J. M. Aristoff, J. T. Horwood, K. T. Alfriend, On a set of J_2 equinoctial orbital elements and their use for uncertainty propagation, *Celestial Mechanics and Dynamical Astronomy* **133** (2021), 1-19.

[6] J. T. Horwood et. al., Beyond covariance realism. A new metric for uncertainty realism, *Signal and Data Processing of Small Targets* **9092** (2014).